1521-0111/12/8201-9–16$25.00
MOLECULAR PHARMACOLOGY
Vol. 82, No. 1
77107/3774484

Mol Pharmacol 82:9–16, 2012

Functional Evaluation of a Fluorescent Schweinfurthin: Mechanism of Cytotoxicity and Intracellular Quantification

Craig H. Kuder, Ryan M. Sheehy, Jeffrey D. Neighbors, David F. Wiemer, and Raymond J. Hohl

Departments of Internal Medicine (C.H.K., R.J.H.), Pharmacology (R.M.S., D.F.W., R.J.H.), and Chemistry (J.D.N., D.F.W.), University of Iowa, Iowa City, Iowa

Received December 6, 2011; accepted March 29, 2012

ABSTRACT

Schweinfurthins are potent inhibitors of cancer cell growth, especially against human central nervous system tumor lines such as SF-295 cells. However, the mechanisms through which these compounds impede cell growth are not fully understood. In an effort to understand the basis for the effects of schweinfurthins, we present a fluorescent schweinfurthin, 3-deoxyschweinfurthin B-like *p*-nitro-bis-stilbene (3dSB-PNBS), which displays biological activity similar to that of 3-deoxyschweinfurthin B (3dSB). These two schweinfurthins retain the unique differential activity of the natural schweinfurthins, as evidenced by the spindle-like morphological changes induced in SF-295 cells and the unaltered appearance of human lung carcinoma A549 cells. We demonstrate that incubation with 3dSB or 3dSB-PNBS results in cleavage of poly-ADP-ribose polymerase (PARP) and caspase-9, both markers of apoptosis. Coincubation of 3dSB or 3dSB-PNBS with the caspase-9 inhibitor (*Z*)-Leu-Glu(*O*-methyl)-His-Asp(*O*-methyl)-fluoromethylketone prevents PARP cleavage. Therapeutic agents that induce apoptosis often activate cellular stress pathways. A marker for multiple stress pathways is the phosphorylation of eukaryotic initiation factor 2α, which is phosphorylated in response to 3dSB and 3dSB-PNBS treatment. Glucose-regulated protein 78 and protein disulfide isomerase, both endoplasmic reticulum chaperones, are up-regulated with schweinfurthin exposure. Using the fluorescent properties of 3dSB-PNBS and dimethoxyphenyl-*p*-nitro-bis-stilbene (DMP-PNBS), a control compound, we show that the intracellular levels of 3dSB-PNBS are higher than those of Rhodamine 123 or DMP-PNBS in SF-295 and A549 cells.

Introduction

Schweinfurthins A, B, and C were isolated from *Macaranga schweinfurthii* collected in western Cameroon and have been investigated for their unique biochemical properties (Beutler et al., 2006). Early evaluation of the natural products demonstrated marked ability to alter mammalian cell growth. For example, in the National Cancer Institute (NCI) 60-cell cancer screen, these compounds displayed differential, potent, growth-inhibitory activities against cells derived from human cancers (Beutler et al., 1998). The most intriguing aspect of schweinfurthin activity is the unique pattern of growth inhibition, in comparison with compounds with known mechanisms of action (Rabow et al., 2002). The best current mechanistic analogy is with (3β,16β)-16-[[2-*O*-acetyl-3-*O*-[2-*O*-(4-methoxybenzoyl)-β-D-xylopyranosyl]-α-L-arabinopyranosyl]oxy]-3,17-dihydroxycholest-5-en-22-one (OSW-1) and the cephalostatin and stellettin families (Neighbors et al., 2006). All of the aforementioned compounds might have previously unexploited targets, which encourages their development as anticancer agents. Further study of the schweinfurthins is attractive because of their marked activity against cancer cell lines, the similarity of their biological activity to that of cephalostatins, and chemical structures that allow for derivatization to related compounds with fluorescent properties.

The cephalostatins cause apoptosis through a novel mechanism that involves endoplasmic reticulum (ER) stress and is

This project was supported by the National Institutes of Health National Cancer Institute [Grant 1R41-CA126020-01] (to Terpenoid Therapeutics), the Roy J. Carver Charitable Trust as a Research Program of Excellence, and the Roland W. Holden Family Program for Experimental Cancer Therapeutics.

Part of this work was presented in partial fulfillment of a doctoral degree: Kuder CH (2009) Schweinfurthins as novel anticancer agents, Ph.D. thesis, University of Iowa, Iowa City, IA.

Article, publication date, and citation information can be found at http://molpharm.aspetjournals.org.

http://dx.doi.org/10.1124/mol.111.077107.

ABBREVIATIONS: NCI, National Cancer Institute; 3dSB-PNBS, 3-deoxyschweinfurthin B-like *p*-nitro bis-stilbene; 3dSB, 3-deoxyschweinfurthin B; PARP, poly-ADP-ribose polymerase; eIF2α, eukaryotic initiation factor 2α; GRP78, glucose-regulated protein 78; PDI, protein disulfide isomerase; ER, endoplasmic reticulum; RIPA, radioimmunoprecipitation assay; UPR, unfolded protein response; DMP-PNBS, 3,4-dimethoxyphenyl *p*-nitro bis-stilbene; Y-27632, (+)-(*R*)-*trans*-4-(1-aminoethyl)-*N*-(4-pyridyl)cyclohexanecarboxamide dihydrochloride; OSW-1, (3β,16β)-16-[[2-*O*-acetyl-3-*O*-[2-*O*-(4-methoxybenzoyl)-β-D-xylopyranosyl]-α-L-arabinopyranosyl]oxy]-3,17-dihydroxy-cholest-5-en-22-one.

independent of apoptosome formation (Dirsch et al., 2003; López-Antón et al., 2006; Rudy et al., 2008). The ER is the major site of secretory and membrane protein synthesis and folding. In unstressed cells, ER chaperones prevent the aggregation of newly synthesized proteins and promote modifications such as disulfide bond formation and glycosylation (Ma and Hendershot, 2004). Mature proteins are transported to their destination, whereas unfolded or poorly folded proteins are targeted for proteasomal degradation (Qu et al., 1996; Werner et al., 1996; Antonny and Schekman, 2001). Disruption of these processes can result in the accumulation of unfolded proteins, leading to ER stress. In response to such disturbances, cells activate pathways aimed at the removal of unfolded or poorly folded protein aggregates, to restore folding equilibrium and to promote survival. This unfolded protein response (UPR) includes the attenuation of protein synthesis through biochemical events including inhibitory phosphorylation of eukaryotic initiation factor 2α (eIF2α) and the upregulation of molecular chaperones such as glucose-regulated protein 78 (GRP78) and protein disulfide isomerase (PDI) (Kozutsumi et al., 1988; Dorner et al., 1989; Rhoads, 1999). These actions decrease the protein load and increase the folding capacity of the ER, respectively. Although the effects of inducing ER stress or the UPR in cancer are relatively unknown, agents that perturb ER function may provide a novel therapeutic strategy (Kim et al., 2008; Huang et al., 2009).

The rarity of the natural schweinfurthins has led to the development of synthetic schemes aimed at their total synthesis (e.g., schweinfurthin B, shown in Fig. 1). Until relatively recently, a scheme for schweinfurthin B synthesis was unknown (Topczewski et al., 2009). Although early attempts failed to yield the natural products, closely related schweinfurthin analogs did provide insight into the structure-function relationships of schweinfurthin-like compounds (Neighbors et al., 2006; Mente et al., 2007, 2008; Ulrich et al., 2010). The left half of the molecule is required for potent biological activity, although some conservative substitutions are allowed (Fig. 1). For example, 3-deoxyschweinfurthin B (3dSB) lacks the A-ring diol but retains potent differential activity (Neighbors et al., 2005). The right half of the molecule is much more amenable to modification, with minimal disruption of biological activity (Kuder et al., 2009). In this context, the fluorescent analog 3-deoxyschweinfurthin B-like *p*-nitro-bis-stilbene (3dSB-PNBS) would be predicted to display biological activity similar to that observed with either schweinfurthin B or 3dSB (Fig. 1). 3,4-Dimethoxyphenyl-*p*-nitro-bis-stilbene (DMP-PNBS) was designed to serve as a control for the active right half (i.e., fluorescent but with reduced biological activity). As postulated, 3dSB-PNBS retains the potent growth-inhibitory activity of the schweinfurthins, whereas DMP-PMBS does not seem to alter cell viability at concentrations up to 10 μM (Topczewski et al., 2010).

Although the ability of the natural compounds to inhibit cancer cell growth has been described, the mechanisms for these activities have yet to be fully elucidated (Holstein et al., 2011). Use of the synthetic schweinfurthins allows better delineation of their biological activity and reveals that growth inhibition is at least partially attributable to apoptosis. We report for the first time that the fluorescent schweinfurthin analog 3dSB-PNBS retains potent biological activity and allows determination of its intracellular concentration.

Materials and Methods

Cell Culture and Materials. SF-295 cells (human glioblastoma multiforme cells) were maintained in RPMI 1640 medium supplemented with 10% fetal bovine serum, 100 units/ml penicillin, 100 μg/ml streptomycin, 2.5 μg/ml amphotericin B, and 2 mM L-glutamine. A549 cells (human lung carcinoma cells) were maintained in Ham's F-12 medium supplemented with 10% fetal bovine serum, 100 units/ml penicillin, 100 μg/ml streptomycin, 2.5 μg/ml amphotericin B, and 2 mM L-glutamine. Both cell lines were incubated at 37°C and 5% CO_2. Thapsigargin, (+)-(*R*)-*trans*-4-(1-aminoethyl)-*N*-(4-pyridyl) cyclohexanecarboxamide dihydrochloride (Y-27632), Rhodamine 123, and etoposide were obtained from Sigma-Aldrich (St. Louis, MO). The caspase-9 inhibitor (*Z*)-Leu-Glu(*O*-methyl)-His-Asp(*O*-methyl)-fluoromethylketone was purchased from MBL International (Woburn, MA). Preparation of the synthetic schweinfurthins has been described previously (Neighbors et al., 2005; Topczewski et al., 2010).

Morphological Staining. Cells were grown on 22- × 22-mm glass coverslips placed in the center of wells in a six-well plate. Treatment with the indicated compounds was performed when cells reached ~65% confluence. At the end of the treatment period, cells were washed twice with phosphate-buffered saline before fixation in 4% paraformaldehyde. Cell membranes were permeabilized in 5-min incubations with 0.2% Triton X-100. After permeabilization, cells underwent blocking with 1% bovine serum albumin for 30 min and then were incubated in Alexa Fluor 633 phallotoxin staining solution (Invitrogen, Carlsbad, CA) for 20 min. Cells were washed and mounted on slides by using Vectashield mounting medium containing 4′,6-diamidino-2-phenylindole (Vector Laboratories, Burlingame, CA). Slides were imaged by using a multiphoton microscope (Bio-Rad Laboratories, Hercules, CA). Images were processed by using ImageJ software (http://rsbweb.nih.gov/ij/).

Propidium Iodide Staining. After reaching ~60% confluence, cells were treated with the indicated compounds. The concentration of etoposide was chosen on the basis of its similarity to 3dSB at 1 μM,

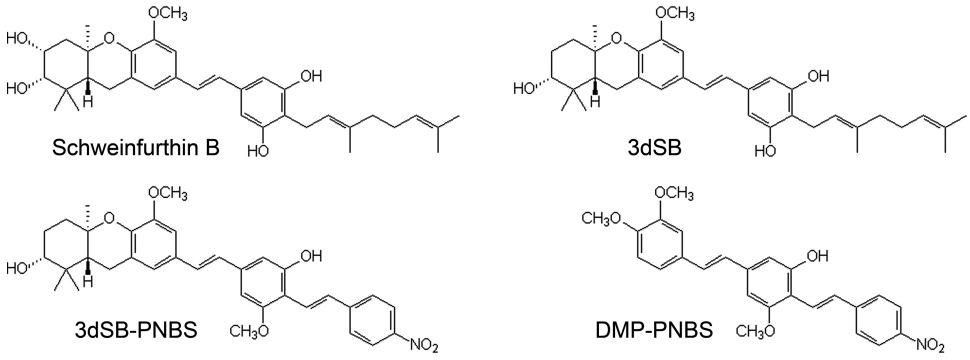

Fig. 1. Structures of the natural product (schweinfurthin B) and synthetic schweinfurthins (3dSB, 3dSB-PNBS, and DMP-PNBS). DMP-PNBS lacks the left-half A- and B-rings, which are necessary for the antiproliferative activity of the schweinfurthins.

in terms of cell viability at 24 h. At the end of the treatment period, both nonadherent and adherent cells were collected and washed. The cells were resuspended in 10 mM HEPES/NaOH, pH 7.4, 150 nM NaCl, 1 mM $MgCl_2$, 5 mM KCl, 1 mM $CaCl_2$. To this cell suspension, 1 μg of propidium iodide (BD Biosciences, San Jose, CA) was added. Flow cytometry was performed immediately with a Becton Dickinson FACScan system (BD Biosciences). Data acquisition and analysis were performed with Cellquest software (BD Biosciences). A bitmap gate was placed around the main population on the basis of forward and side light scatter, to exclude debris and aggregates but to include dead, dying, and viable cells. A total of 10,000 events that satisfied this gate were collected in listmode. Propidium iodide emission data were collected in the FL2 channel through the standard 585/42 bandpass filter. Cell death percentages were calculated by subtracting the percentage of viable cells from the percentage of total events (100%).

Western Blot Analysis. Cells were lysed in radioimmunoprecipitation assay (RIPA) buffer [0.15 M NaCl, 0.05 M Tris HCl, 1% (w/v) sodium deoxycholate, 0.1% (w/v) SDS, 1% (v/v) Triton X-100, 1 mM EDTA, pH 7.4] containing 1 mM sodium vanadate, 10 mM sodium fluoride, 2.5 mM phenylmethylsulfonyl fluoride, and protease inhibitor cocktail (Sigma-Aldrich). Protein levels were quantified with the bicinchoninic acid method (Smith et al., 1985). Equal protein quantities were resolved with SDS-polyacrylamide gel electrophoresis and were transferred to a polyvinylidene fluoride membrane. Membranes were blocked with 5% milk in Tris-buffered saline/Tween 20. Primary antibodies were incubated with the membranes for 1 h for poly-ADP-ribose polymerase (PARP), PDI, GRP78, or β-tubulin (Santa Cruz Biotechnology, Santa Cruz, CA) or overnight for phosphorylated eIF2α, eIF2α, or caspase-9 (Cell Signaling Technology, Danvers, MA). Membranes were incubated with appropriate secondary antibodies for 1 h, and protein levels were detected with an enhanced chemiluminescence detection kit (GE Healthcare, Chalfont St. Giles, Buckinghamshire, UK).

Compound Fluorometric Quantification. SF-295 or A549 cells were plated in six-well plates. At approximately 60 to 70% confluence, cells were incubated in the presence or absence of 3dSB-PNBS, DMP-PNBS, or Rhodamine 123, as described. After 24 h of incubation, cells were washed once before incubation in 0.25% trypsin/EDTA solution for 5 min. Trypsin was immediately neutralized with an equal volume of medium. Cells were collected and subjected to centrifugation at 1500*g* for 7 min at 4°C. The cell pellet was washed once with phosphate-buffered saline, and cells were lysed on ice with RIPA lysis buffer (described above). After 30 min, the lysate was cleared through centrifugation at 14,000*g* for 15 min at 4°C. The protein content of each sample was determined by using the bicinchoninic acid assay. Lysates were stored at −80°C before fluorometric analysis. The relative fluorescence of each sample was measured by using a SpectraMax M2^e microplate reader (Molecular Devices, Sunnyvale, CA). Relative fluorescence levels were determined at the excitation and emission maxima for each compound. Sample values were calculated on the basis of linear, five-point, standard curves. Standard curves were generated with five concentrations of compound diluted in RIPA buffer. Values obtained from fluorometric analysis were normalized with respect to sample protein concentrations.

Statistical Analysis. To determine the statistical significance of flow cytometric and intracellular localization studies, two-tailed t testing with the α value set at the 0.05 level of significance was applied.

Results

Schweinfurthin Analogs Retain Differential Activity. The feature that prompted initial interest in the schweinfurthins was their ability to inhibit cell growth in selective human central nervous system tumor cell lines. To evaluate the selective activities of 3dSB, 3dSB-PNBS, and DMP-PNBS after 48 h of exposure, cell morphological features of a schweinfurthin-sensitive cell line (i.e., SF-295 cells) and a relatively resistant cell line (i.e., A549 cells) were examined. Previous studies demonstrated that schweinfurthin activity alters cell morphological features; specifically, cells become spindle-like (Chi et al., 2009; Kuder et al., 2009; Turbyville et al., 2010). After 48 h of exposure to 3dSB or 3dSB-PNBS, SF-295 cells became spindle-shaped and exhibited phalloidin staining predominantly at the peripheral edges of the cells, whereas cells exposed to DMP-PNBS appeared similar to control cells (Fig. 2A). Treatment with the Rho-associated protein kinase inhibitor Y-27632 did not induce the same morphological changes, which supports the hypothesis that the mechanism of schweinfurthin activity is not mediated exclusively by Rho-associated protein kinase activity. To examine further the differences in sensitivity between cell lines, the effects on the morphological features of A549 cells were examined. After 48 h of treatment with 3dSB-PNBS or 3dSB, A549 cells displayed minimal changes in phalloidin staining or cellular shape (Fig. 2B). Likewise, DMP-PNBS did not seem to alter A549 cell morphological features at a concentration of 1 μM. However, treatment with Y-27632 induced changes in A549 cell morphological features that appeared similar to the changes demonstrated with the SF-295 cell line. The sensitivity differences between SF-295 and A549 cells with respect to treatment with 3dSB and 3dSB-PNBS accentuated the compounds' schweinfurthin-like activity.

3dSB and 3dSB-PNBS Induce Apoptosis. As established inhibitors of cancer cell growth, schweinfurthins might elicit their effects through several mechanisms, such as cell cycle arrest, decreased growth signaling, cell senescence, and/or cell death. On the basis of observed changes in cell morphological features (Fig. 2) and increased levels of cellular debris that accompanied schweinfurthin treatment

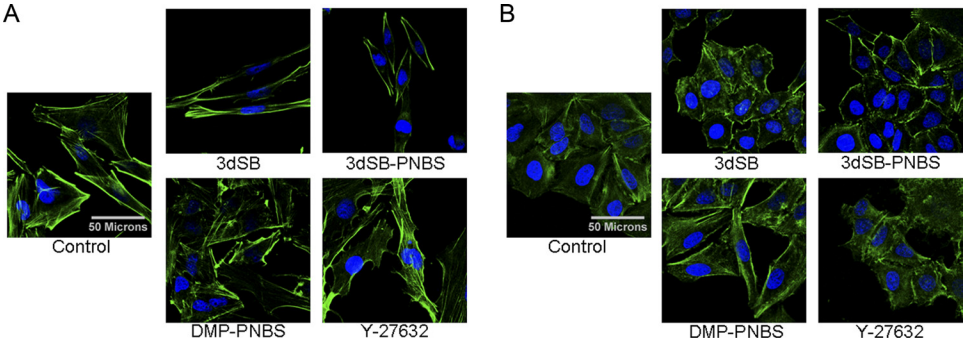

Fig. 2. A, effects of schweinfurthin treatment on phalloidin staining in SF-295 cells. In this experiment, cells were left untreated (Control) or were treated with 3dSB (500 nM), 3dSB-PNBS (500 nM), DMP-PNBS (1 μM), or Y-27632 (10 μM) for 48 h. Cells were stained with 4′,6-diamidino-2-phenylindole (blue) and phalloidin (green). B, effects of schweinfurthin treatment on phalloidin staining in A549 cells. A549 cells were left untreated (Control) or were treated with 3dSB (500 nM), 3dSB-PNBS (500 nM), DMP-PNBS (1 μM), or Y-27632 (10 μM) for 48 h. Staining conditions were as described for A.

(data not shown), cell death was suspected. To investigate this hypothesis, effects on markers of apoptosis were examined. In SF-295 cells, 3dSB treatment led to concentration- and time-dependent increases in cell death (Fig. 3, A and B). Treatment with the topoisomerase II inhibitor etoposide caused an increase in cell death rates, consistent with its cytotoxicity. The fluorescent properties of 3dSB-PNBS precluded its analysis in this assay.

Cell death usually occurs as a consequence of apoptosis induction or necrosis. Apoptosis can be detected on the basis of PARP cleavage, which is a universal downstream target of apoptotic signaling cascades. Treatment with 3dSB-PNBS or 3dSB did not induce PARP cleavage or apoptosis by 24 h, a finding consistent with previous studies that indicated limited toxicity at 24 h with similar concentrations (Fig. 3B) (Kuder et al., 2009). At 36 h, however both of these compounds induced PARP cleavage, whereas DMP-PNBS did not (Fig. 3B). Consistent with its known role in apoptotic cell death, treatment with etoposide led to PARP cleavage by 24 h (Karpinich et al., 2002). These results demonstrated that schweinfurthin treatment led to the induction of apoptosis in SF-295 cells.

Caspase-9 Inhibition Reverses 3dSB- and 3dSB-PNBS-Induced PARP Cleavage. Cleavage and activation of caspase proteins represent a crucial step in the execution of many apoptotic pathways. Each apoptotic signaling pathway engages specific caspases. Caspase-9 has a prominent role in the initiation of intrinsic apoptosis (Johnson and Jarvis, 2004). Treatment with either 3dSB or 3dSB-PNBS induced the cleavage of caspase-9 by 24 h, whereas DMP-PNBS failed to produce cleavage at all time points tested (Fig. 4A). Etoposide caused caspase-9 cleavage by 24 h. To assess the role of caspase-9 in schweinfurthin-induced apoptosis, PARP cleavage was evaluated in schweinfurthin-treated cells with or without the caspase-9 inhibitor (*Z*)-Leu-Glu(*O*-methyl)-His-Asp(*O*-methyl)-fluoromethylketone (Fig. 4B). Caspase-9 inhibition reversed 3dSB- and 3dSB-PNBS-induced PARP cleavage at 36 h. The caspase-9 inhibitor also reversed etoposide-induced PARP cleavage at 36 h (Fig. 4B).

3dSB and 3dSB-PNBS Trigger Phosphorylation of eIF2α and Increase Expression of GRP78 and PDI. The disruption of ER protein-folding capacity by therapeutic agents and cellular events results in the accumulation of unfolded proteins and ER stress. To restore ER homeostasis, stressed cells induce UPR signaling cascades. A key component of this response is the reduction of protein synthesis, which serves to reduce the protein load. Inhibition of protein synthesis is achieved through phosphorylation of eIF2α. Treatment with 3dSB or 3dSB-PNBS induced phosphorylation of eIF2α by 9 h after exposure; phosphorylation persisted

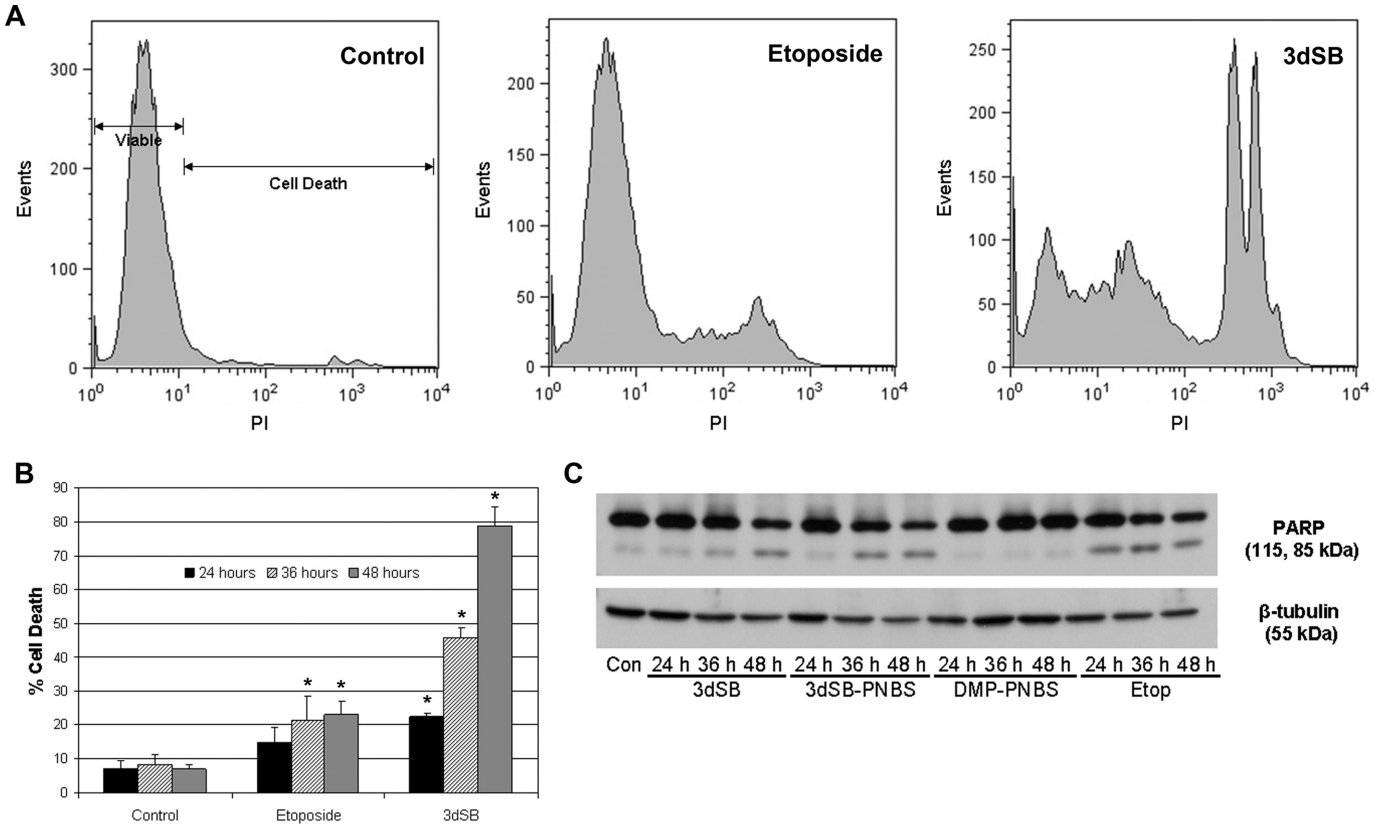

Fig. 3. Induction of apoptosis by 3dSB and 3dSB-PNBS. A and B, effects of 3dSB treatment on cell viability. A, representative histograms of propidium iodide (PI) staining in SF-295 cells treated with or without 3dSB (1 μM) or etoposide (50 μM) for 48 h. Propidium iodide staining was evaluated with flow cytometry, as described under *Materials and Methods*. B, quantification with flow cytometry of propidium iodide staining in cells after 24, 36, or 48 h of incubation with or without 3dSB (1 μM) or etoposide (50 μM). Propidium iodide staining was performed as described for A. Values are presented as the percentages of dead cells (mean $\pm$ S.D.) from triplicate treatments. $*$, $p < 0.05$, as determined with a two-tailed t test comparing treatment and control groups. This experiment is representative of three independent experiments. C, effects of schweinfurthin treatment on PARP cleavage. Western blot analysis of SF-295 cells left untreated (Con) or treated with 3dSB (1 μM), 3dSB-PNBS (1 μM), DMP-PNBS (10 μM), or etoposide (Etop) (50 μM) for the indicated times was performed. PARP cleavage and β-tubulin (loading control) blotting were performed as indicated under *Materials and Methods*.

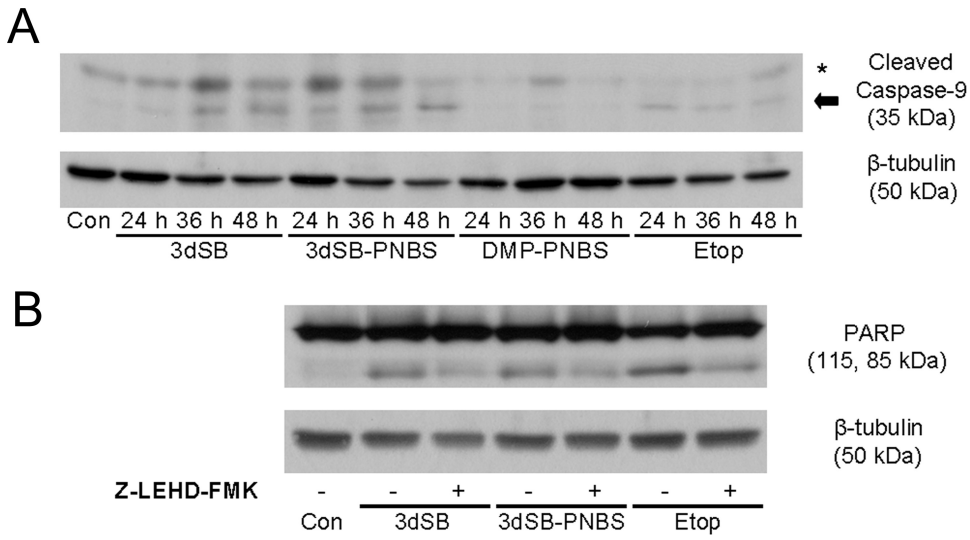

Fig. 4. Inhibition of 3dSB- and 3dSB-PNBS-induced caspase-9 cleavage and reversal of PARP cleavage. A, effects of schweinfurthin treatment on caspase-9 cleavage. Western blot analysis of SF-295 cells left untreated (Con) or treated with 3dSB (1 μM), 3dSB-PNBS (1 μM), DMP-PNBS (10 μM), or etoposide (Etop) (50 μM) for the indicated times was performed. Blots were probed with antibodies to cleaved caspase-9 and β-tubulin. *, nonspecific band. Arrow, cleaved caspase-9. B, effects of caspase-9 inhibition on schweinfurthin-induced apoptosis. SF-295 cells were left untreated or were treated with 3dSB (1 μM), 3dSB-PNBS (1 μM), or etoposide (50 μM), with or without the caspase-9 inhibitor (*Z*)-Leu-Glu(*O*-methyl)-His-Asp(*O*-methyl)-fluoromethylketone (Z-LEHD-FMK) (50 μM), for 36 h. Blots were probed with anti-PARP and anti-β-tubulin antibodies. Experiments were performed in triplicate.

between 9 and 24 h, with peak phosphorylation levels occurring at approximately 14 h (Fig. 5A). At 14 h, 3dSB and DMP-PNBS increased the phosphorylation of eIF2α, normalized with respect to eIF2α levels, by ~4-fold. The eIF2α phosphorylation levels induced by 3dSB and 3dSB-PNBS were similar to those observed with thapsigargin, a sarcoplasmic reticulum Ca^{2+}-ATPase inhibitor. The analog DMP-PNBS did not increase the phosphorylation of eIF2α (Fig. 5A).

In addition to halting protein synthesis, cells experiencing ER stress up-regulate molecular chaperones such as GRP78 and PDI, in an effort to alleviate stress and to restore normal function. Both 3dSB and 3dSB-PNBS treatment induced increases in GRP78 expression between 1 and 3 h (Fig. 5, B and C). This initial GRP78 increase was not sustained; levels returned to control levels by 6 h before increasing again by 14 h. This secondary increase was sustained through 24 h with 3dSB, whereas GRP78 expression returned to control levels by 24 h with 3dSB-PNBS treatment. DMP-PNBS induced a slight increase in GRP78 expression by 14 h, which persisted through 18 h (Fig. 5B). PDI is a molecular chaperone involved in the formation of disulfide bonds in nascent peptides. The expression level of this molecular chaperone

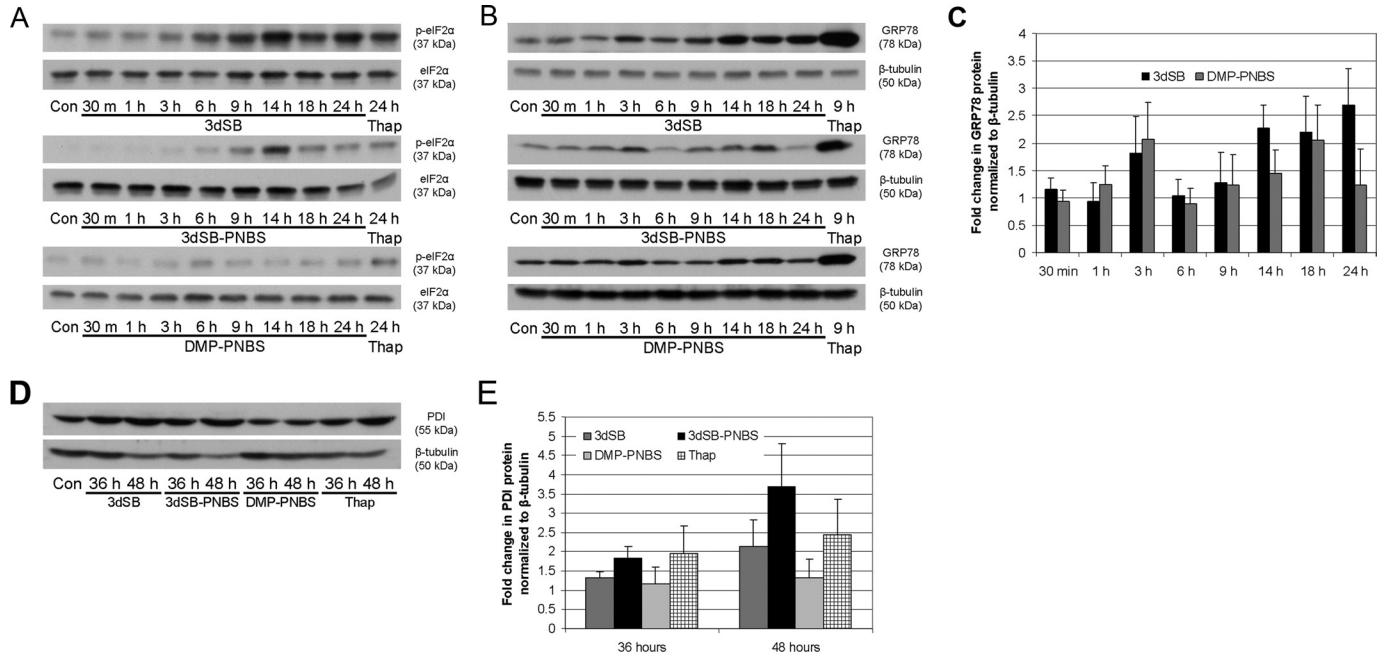

Fig. 5. Induction of eIF2α phosphorylation and up-regulation of GRP78 and PDI by 3dSB and 3dSB-PNBS. A, time course of eIF2α phosphorylation. SF-295 cells were left untreated (Con) or were treated with 3dSB (1 μM), 3dSB-PNBS (1 μM), or DMP-PNBS (10 μM) for the indicated times (30 min to 24 h). As a positive control, cells were treated with thapsigargin (Thap) (5 μM) for 24 h. B, time course of GRP78 expression. SF-295 cells were treated as in A with the exception of thapsigargin, which was treated for 9 h. Blots were probed with anti-GRP78 and anti-β-tubulin antibodies. C, quantification of GRP78 protein levels, normalized with respect to β-tubulin levels, after incubation with 3dSB (1 μM) or 3dSB-PNBS (1 μM) for times ranging from 30 min to 24 h. The graph displays GRP78 protein levels (mean ± S.D.) from three independent experiments. D, effects of schweinfurthin treatment on PDI expression. SF-295 cells were left untreated (Con) or were treated with 3dSB (1 μM), 3dSB-PNBS (1 μM), DMP-PNBS (10 μM), or thapsigargin (5 μM) for 36 or 48 h. Blots were probed with anti-PDI and anti-β-tubulin antibodies. E, quantification of PDI levels, normalized with respect to β-tubulin levels, after incubation with 3dSB (1 μM), 3dSB-PNBS (1 μM), DMP-PNBS (10 μM), or thapsigargin (5 μM) for 36 or 48 h. The graph displays PDI protein levels (mean ± S.D.) from three independent experiments.

was increased by 36 h with 3dSB-PNBS and thapsigargin (Fig. 5, D and E). After 48 h of incubation, PDI expression was increased by 3dSB, 3dSB-PNBS, and thapsigargin. This increase was consistent with the increased expression of molecular chaperones induced by ER stress. Treatment with DMP-PNBS did not induce an appreciable change in PDI levels (Fig. 5, D and E).

Intracellular Concentrations of 3dSB-PNBS Are Higher than Those of DMP-PNBS. The fluorescent schweinfurthin 3dSB-PNBS has structural characteristics that result in fluorescence without disruption of its cellular activity. This compound has an excitation maximum of 419 nm and an emission maximum of 560 nm. DMP-PNBS also exhibits fluorescent properties, with maximal excitation and emission wavelengths of 421 nm and 579 nm, respectively. Compound fluorescence was used to determine intracellular concentrations and to define differences between 3dSB-PNBS and DMP-PNBS. It is noteworthy that the intracellular concentrations of 3dSB-PNBS were 12- to 15-fold higher than those of DMP-PNBS or Rhodamine 123 in SF-295 and A549 cells (Fig. 6). The concentrations of DMP-PNBS and Rhodamine 123 were similar in both cell lines.

Discussion

Schweinfurthins are inhibitors of cell growth, but the sites and targets of their actions are unknown. To address such issues, structural manipulations that yield valuable properties such as fluorescence are often explored. One prominent example of this approach is the design and creation of fluorescent analogs of paclitaxel (Taxol), which have proven useful for defining the mechanistic details of tubulin interactions (Sengupta et al., 1995; Díaz et al., 2000). The development of fluorescent compounds is worthwhile only if such compounds retain the activity of the class of compounds being investigated. We demonstrated that the fluorescent schweinfurthin 3dSB-PNBS retained the differential activity displayed by schweinfurthin B and 3dSB, which validates its use. This differential activity was confirmed by increased sensitivity of SF-295 cells to 3dSB-PNBS, in comparison with A549 cells, as assayed with cytotoxic and morphological measures (Topczewski et al., 2010) (Fig. 2). Differential activities of these agents were confirmed with other cell lines from the NCI 60-cell screen, including the U251 and OVCAR-5 cell lines (data not shown). The fluorescent compound lacking the tricyclic left half of the schweinfurthin core, DMP-PNBS, did not exhibit biological activity in the SF-295 or A549 cell lines but did have fluorescent properties similar to those of 3dSB-PNBS.

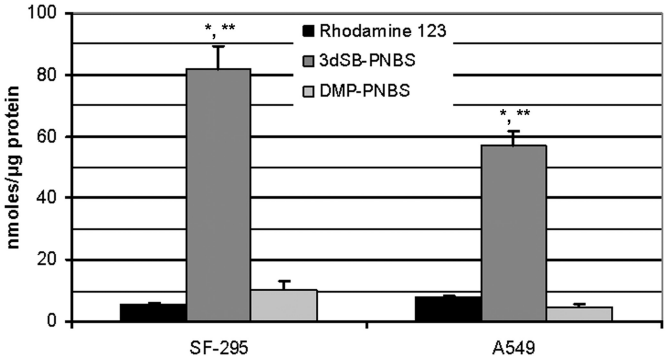

Fig. 6. Intracellular concentrations of 3dSB-PNBS in comparison with Rhodamine 123 or DMP-PNBS. SF-295 or A549 cells were incubated with or without 3dSB-PNBS, DMP-PNBS, or Rhodamine 123, at a concentration of 500 nM, for 24 h. Intracellular concentrations were determined as described under *Materials and Methods*. The graph represents one of three experiments performed in triplicate. Bars, average intracellular concentrations normalized with respect to protein content; error bars, S.D. *, $p < 0.05$, as determined with a two-tailed t test comparing 3dSB-PNBS and Rhodamine 123. **, $p < 0.05$, as determined with a two-tailed t test comparing 3dSB-PNBS and DMP-PNBS.

Growth inhibition often is caused by cell cycle arrest or cell death. After treatment with 3dSB or 3dSB-PNBS at concentrations sufficient to produce growth inhibition, cellular debris levels were noticeably increased (data not shown). On the basis of this observation, it was hypothesized that the cellular debris was the result of cell death. Indeed, treatment with 3dSB led to a marked increase in the percentage of dead cells, which might be caused by apoptosis or necrosis (Fig. 3A). Schweinfurthin-induced cell death is at least partly dependent on apoptosis, as demonstrated by the cleavage of PARP with 3dSB and 3dSB-PNBS treatment (Fig. 3B). As expected, DMP-PNBS did not induce apoptosis at the concentrations tested. Caspase-9 is an initiator caspase that is commonly cleaved and activated during intrinsic apoptotic signaling (Fulda and Debatin, 2006). Schweinfurthin treatment led to cleavage of caspase-9, which suggests that this caspase participates in schweinfurthin-induced apoptosis (Fig. 4A). Inhibition of caspase-9 activity reversed schweinfurthin-induced PARP cleavage, which suggests that apoptosis is at least partly dependent on caspase-9 activity (Fig. 4B).

The growth-inhibitory activity of the schweinfurthins in the NCI 60-cell assay is positively correlated with that of another family of natural products, the cephalostatins (Neighbors et al., 2006). Cephalostatin 1 and 2 were shown to induce ER stress, resulting in caspase-9 activity and apoptosis (López-Antón et al., 2006). Several compounds are known to induce ER stress as part of their biological actions; among these are a sarcoplasmic/endoplasmic reticulum Ca^{2+}-ATPase inhibitor (thapsigargin), an inhibitor of glycosylation (tunicamycin), an inhibitor of ER-Golgi trafficking (brefeldin A), and a proteasomal inhibitor (bortezomib) (Price et al., 1992; Obeng et al., 2006). Similar to the effects of these agents, schweinfurthin treatment caused the phosphorylation of eIF2α and increased expression of ER chaperones PDI and GRP78 (Fig. 5). Although schweinfurthin treatment induced components of the UPR, the changes in GRP78 expression were blunted, in comparison with thapsigargin treatment (Fig. 5B). This may indicate that ER stress is not the immediate biochemical response to the schweinfurthins. The role of ER stress in the induction of apoptosis can involve several different mechanisms, such as apoptosis signal-regulating kinase 1 signaling (Ichijo et al., 1997), capase-12/caspase-4 cleavage (Hitomi et al., 2004), and growth arrest and DNA damage-inducible gene 153 activity (Zinszner et al., 1998). Schweinfurthin-induced apoptosis may be dependent on these processes or may involve a novel apoptotic mechanism, much like the cephalostatins (Dirsch et al., 2003; Müller et al., 2005; López-Antón et al., 2006; Rudy et al., 2008).

The fluorescent schweinfurthin analog 3dSB-PNBS displayed biological activity similar to that of 3dSB in all assays examined, which justifies its use for determination of localization and intracellular concentrations (Figs. 2–5). We have described differences in the localization of 3dSB-PNBS and DMP-PNBS in SF-295 cells (Topczewski et al., 2010). These

compounds also displayed differences in intracellular concentrations. The intracellular concentrations of 3dSB-PNBS were 12- to 15-fold greater than those of DMP-PNBS in SF-295 and A549 cells (Fig. 6). The disparity between 3dSB-PNBS and DMP-PNBS might be attributable to sequestration of target binding; however, differences in cellular uptake and efflux also might contribute. Although there were differences in the intracellular concentrations of 3dSB-PNBS in SF-295 and A549 cells, these differences cannot be fully appreciated without determination of the cellular volume of both cell lines. Because they are potential therapeutic agents for central nervous system-derived malignancies, the capacity of the schweinfurthins to traverse the blood-brain barrier is a key factor in their development. On the basis of the techniques described here, 3dSB-PNBS could be used to test blood-brain barrier penetrance in vitro and in vivo, as well as schweinfurthin uptake and efflux (Lelong et al., 1991; Miller et al., 2000).

The correlation between schweinfurthin and cephalostatin activity in the NCI 60-cell cancer screen is intriguing with respect to the potential targets of these natural products. The structures of these families are quite different, but their activities seem to be somewhat similar. The activities of the schweinfurthins and cephalostatins do not appear similar to those of compounds with known mechanisms of action; this assertion is supported by studies that suggest a novel mechanism for cephalostatin-induced apoptosis (Dirsch et al., 2003; López-Antón et al., 2006; Rudy et al., 2008). Because of their unique activities, these compounds may represent a novel class of anticancer agents. The ability to synthesize fluorescent analogs that retain the biological activity of the schweinfurthins provides new possibilities in the investigation of this potentially unique mechanism.

Acknowledgments

We thank Joseph J. Topczewski for assistance with the preparation of fluorescent compounds, the University of Iowa Flow Cytometry Facility (Iowa City, IA), and the University of Iowa Central Microscopy Research Facilities (Iowa City, IA).

Authorship Contributions

Participated in research design: Kuder, Sheehy, Neighbors, and Hohl.

Conducted experiments: Kuder, Sheehy, and Neighbors.

Contributed new reagents or analytic tools: Neighbors and Wiemer.

Performed data analysis: Kuder, Sheehy, Neighbors, Wiemer, and Hohl.

Wrote or contributed to the writing of the manuscript: Kuder, Sheehy, Neighbors, Wiemer, and Hohl.

References

Antonny B and Schekman R (2001) ER export: public transportation by the COPII coach. *Curr Opin Cell Biol* **13:**438–443.

Beutler JA, Jato JG, Cragg G, Wiemer DF, Neighbors JD, Salnikova M, Hollingshead M, Scudiero DA, and McCloud TG (2006) The schweinfurthins: issues in the development of a plant-derived anticancer lead, in *Medicinal and Aromatic Plants: Agricultural, Commercial, Ecological, Legal, Pharmacological and Social Aspects* (Bogers RJ, Craker LE, and Lange D eds) pp 301–309, Springer, Dordrecht, The Netherlands.

Beutler JA, Shoemaker RH, Johnson T, and Boyd MR (1998) Cytotoxic geranyl stilbenes from *Macaranga schweinfurthii*. *J Nat Prd* **61:**1509–1512.

Cui C, JaJa J, Turbyville T, Beutler J, Gudla P, Nandy K, and Lockett S (2009) Quantifying the astrocytoma cell response to candidate pharmaceutical from F-ACTIN image analysis, in *Engineering in Medicine and Biology Society, 2009. Annual International Conference of the IEEE*; 2009 Sep 2–6; Minneapolis, MN. pp 5768–5771, http://dx.doi.org/10.1109/IEMBS.2009.5332528.

Díaz JF, Strobe R, Engelborghs Y, Souto AA, and Andreu JM (2000) Molecular recognition of taxol by microtubules. Kinetics and thermodynamics of binding of fluorescent taxol derivatives to an exposed site. *J Biol Chem* **275:**26265–26276.

Dirsch VM, Müller IM, Eichhorst ST, Pettit GR, Kamano Y, Inoue M, Xu JP, Ichihara Y, Wanner G, and Vollmar AM (2003) Cephalostatin 1 selectively triggers the release of Smac/DIABLO and subsequent apoptosis that is characterized by an increased density of the mitochondrial matrix. *Cancer Res* **63:**8869–8876.

Dorner AJ, Wasley LC, and Kaufman RJ (1989) Increased synthesis of secreted proteins induces expression of glucose-regulated proteins in butyrate-treated Chinese hamster ovary cells. *J Biol Chem* **264:**20602–20607.

Fulda S and Debatin KM (2006) Extrinsic versus intrinsic apoptosis pathways in anticancer chemotherapy. *Oncogene* **25:**4798–4811.

Hitomi J, Katayama T, Eguchi Y, Kudo T, Taniguchi M, Koyama Y, Manabe T, Yamagishi S, Bando Y, Imaizumi K, et al. (2004) Involvement of caspase-4 in endoplasmic reticulum stress-induced apoptosis and Aβ-induced cell death. *J Cell Biol* **165:**347–356.

Holstein SA, Kuder CH, Tong H, and Hohl RJ (2011) Pleiotropic effects of a schweinfurthin on isoprenoid homeostasis. *Lipids* **46:**907–921.

Huang WC, Lin YS, Chen CL, Wang CY, Chiu WH, and Lin CF (2009) Glycogen synthase kinase-3β mediates endoplasmic reticulum stress-induced lysosomal apoptosis in leukemia. *J Pharmacol Exp Ther* **329:**524–531.

Ichijo H, Nishida E, Irie K, ten Dijke P, Saitoh M, Moriguchi T, Takagi M, Matsumoto K, Miyazono K, and Gotoh Y (1997) Induction of apoptosis by ASK1, a mammalian MAPKKK that activates SAPK/JNK and p38 signaling pathways. *Science* **275:**90–94.

Johnson CR and Jarvis WD (2004) Caspase-9 regulation: an update. *Apoptosis* **9:**423–427.

Karpinich NO, Tafani M, Rothman RJ, Russo MA, and Farber JL (2002) The course of etoposide-induced apoptosis from damage to DNA and p53 activation to mitochondrial release of cytochrome *c*. *J Biol Chem* **277:**16547–16552.

Kim I, Xu W, and Reed JC (2008) Cell death and endoplasmic reticulum stress: disease relevance and therapeutic opportunities. *Nat Rev Drug Discov* **7:**1013–1030.

Kozutsumi Y, Segal M, Normington K, Gething MJ, and Sambrook J (1988) The presence of malfolded proteins in the endoplasmic reticulum signals the induction of glucose-regulated proteins. *Nature* **332:**462–464.

Kuder CH, Neighbors JD, Hohl RJ, and Wiemer DF (2009) Synthesis and biological activity of a fluorescent schweinfurthin analogue. *Bioorg Med Chem* **17:**4718–4723.

Lelong IH, Guzikowski AP, Haugland RP, Pastan I, Gottesman MM, and Willingham MC (1991) Fluorescent verapamil derivative for monitoring activity of the multidrug transporter. *Mol Pharmacol* **40:**490–494.

López-Antón N, Rudy A, Barth N, Schmitz ML, Schmitz LM, Pettit GR, Schulze-Osthoff K, Dirsch VM, and Vollmar AM (2006) The marine product cephalostatin 1 activates an endoplasmic reticulum stress-specific and apoptosome-independent apoptotic signaling pathway. *J Biol Chem* **281:**33078–33086.

Ma Y and Hendershot LM (2004) ER chaperone functions during normal and stress conditions. *J Chem Neuroanat* **28**:51–65.

Mente NR, Neighbors JD, and Wiemer DF (2008) BF3 $\times$ Et_2O-mediated cascade cyclizations: synthesis of schweinfurthins F and G. *J Org Chem* **73:**7963–7970.

Mente NR, Wiemer AJ, Neighbors JD, Beutler JA, Hohl RJ, and Wiemer DF (2007) Total synthesis of (*R*,*R*,*R*)- and (*S*,*S*,*S*)-schweinfurthin F: differences of bioactivity in the enantiomeric series. *Bioorg Med Chem Lett* **17:**911–915.

Miller DS, Nobmann SN, Gutmann H, Toeroek M, Drewe J, and Fricker G (2000) Xenobiotic transport across isolated brain microvessels studied by confocal microscopy. *Mol Pharmacol* **58:**1357–1367.

Müller IM, Dirsch VM, Rudy A, López-Antón N, Pettit GR, and Vollmar AM (2005) Cephalostatin 1 inactivates Bcl-2 by hyperphosphorylation independent of M-phase arrest and DNA damage. *Mol Pharmacol* **67:**1684–1689.

Neighbors JD, Beutler JA, and Wiemer DF (2005) Synthesis of nonracemic 3-deoxyschweinfurthin B. *J Org Chem* **70:**925–931.

Neighbors JD, Salnikova MS, Beutler JA, and Wiemer DF (2006) Synthesis and structure-activity studies of schweinfurthin B analogs: evidence for the importance of a D-ring hydrogen bond donor in expression of differential cytotoxicity. *Bioorg Med Chem* **14:**1771–1784.

Obeng EA, Carlson LM, Gutman DM, Harrington WJ Jr, Lee KP, and Boise LH (2006) Proteasome inhibitors induce a terminal unfolded protein response in multiple myeloma cells. *Blood* **107:**4907–4916.

Price BD, Mannheim-Rodman LA, and Calderwood SK (1992) Brefeldin A, thapsigargin, and AlF_4^- stimulate the accumulation of GRP78 mRNA in a cycloheximide dependent manner, whilst induction by hypoxia is independent of protein synthesis. *J Cell Physiol* **152:**545–552.

Qu D, Teckman JH, Omura S, and Perlmutter DH (1996) Degradation of a mutant secretory protein, α1-antitrypsin Z, in the endoplasmic reticulum requires proteasome activity. *J Biol Chem* **271:**22791–22795.

Rabow AA, Shoemaker RH, Sausville EA, and Covell DG (2002) Mining the National Cancer Institute's tumor-screening database: identification of compounds with similar cellular activities. *J Med Chem* **45:**818–840.

Rhoads RE (1999) Signal transduction pathways that regulate eukaryotic protein synthesis. *J Biol Chem* **274:**30337–30340.

Rudy A, López-Antón N, Barth N, Pettit GR, Dirsch VM, Schulze-Osthoff K, Rehm M, Prehn JH, Vogler M, Fulda S, et al. (2008) Role of Smac in cephalostatin-induced cell death. *Cell Death Differ* **15:**1930–1940.

Sengupta S, Boge TC, Georg GI, and Himes RH (1995) Interaction of a fluorescent paclitaxel analog with tubulin. *Biochemistry* **34:**11889–11894.

Smith PK, Krohn RI, Hermanson GT, Mallia AK, Gartner FH, Provenzano MD, Fujimoto EK, Goeke NM, Olson BJ, and Klenk DC (1985) Measurement of protein using bicinchoninic acid. *Anal Biochem* **150:**76–85.

Topczewski JJ, Kuder CH, Neighbors JD, Hohl RJ, and Wiemer DF (2010) Fluores-

cent schweinfurthin B and F analogs with anti-proliferative activity. *Bioorg Med Chem* **18:**6734–6741.
Topczewski JJ, Neighbors JD, and Wiemer DF (2009) Total synthesis of (+)-schweinfurthins B and E. *J Org Chem* **74:**6965–6972.
Turbyville TJ, Gürsel DB, Tuskan RG, Walrath JC, Lipschultz CA, Lockett SJ, Wiemer DF, Beutler JA, and Reilly KM (2010) Schweinfurthin A selectively inhibits proliferation and Rho signaling in glioma and neurofibromatosis type 1 tumor cells in a NF1-GRD–dependent manner. *Mol Cancer Ther* **9:**1234–1243.
Ulrich NC, Kodet JG, Mente NR, Kuder CH, Beutler JA, Hohl RJ, and Wiemer DF (2010) Structural analogues of schweinfurthin F: probing the steric, electronic, and hydrophobic properties of the D-ring substructure. *Bioorg Med Chem* **18:**1676–1683.
Werner ED, Brodsky JL, and McCracken AA (1996) Proteasome-dependent endoplasmic reticulum-associated protein degradation: an unconventional route to a familiar fate. *Proc Natl Acad Sci U S A* **93:**13797–13801.
Zinszner H, Kuroda M, Wang X, Batchvarova N, Lightfoot RT, Remotti H, Stevens JL, and Ron D (1998) CHOP is implicated in programmed cell death in response to impaired function of the endoplasmic reticulum. *Genes Dev* **12:**982–995.

Address correspondence to: Raymond J. Hohl, University of Iowa, SE 313 GH, Iowa City, IA 52242. E-mail: raymond-hohl@uiowa.edu